iScience

CellPress
OPEN ACCESS

Article

Biochemical profiling of the protein encoded by grass carp reovirus genotype II

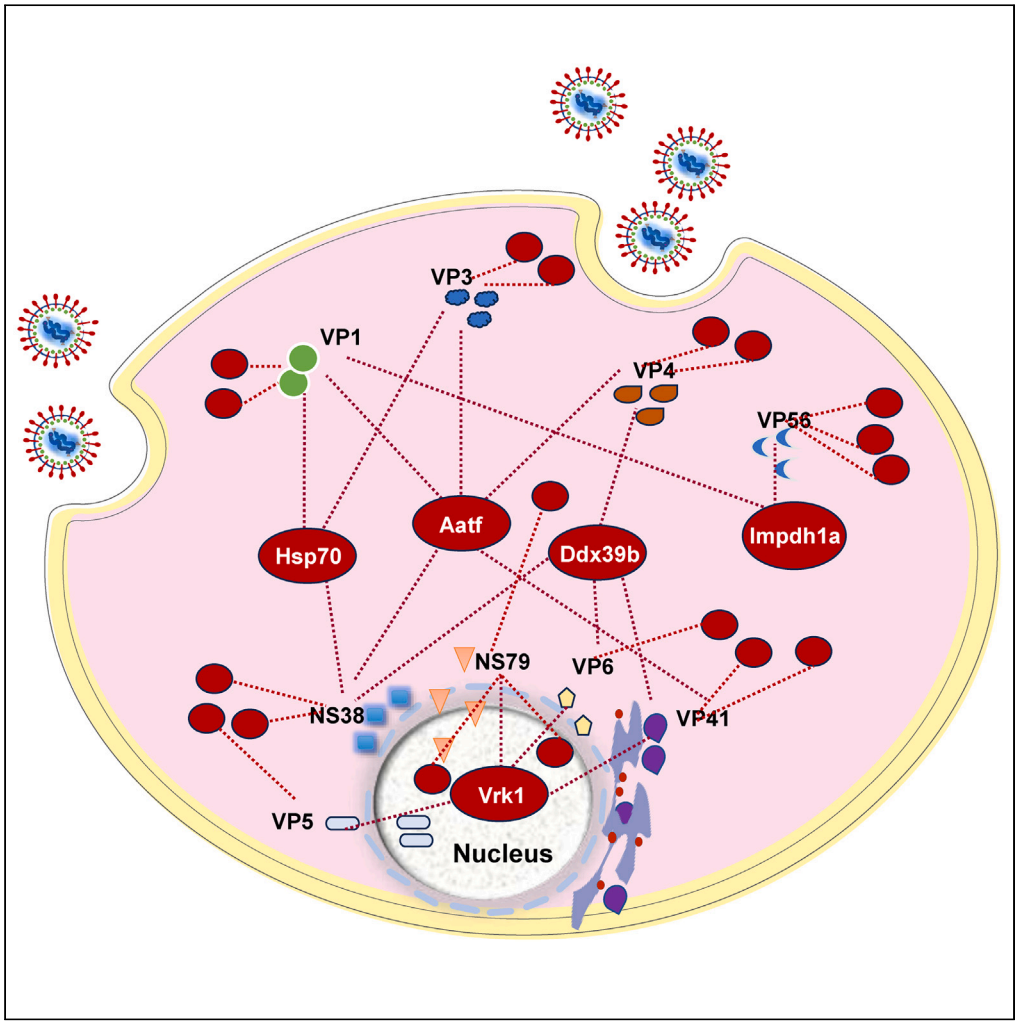

Man Liu, Chen Xu, Yong Zhou, ..., Wenzhi Liu, Xianghui Kong, Yuding Fan

xhkong@htu.cm (X.K.)
fanyd@yfi.ac.cn (Y.F.)

Highlights

A highly lethal strain of GCRV-II, GCRV-DY197, was isolated and sequenced

A GCRV-host protein interaction network was built in GCO cell line

PTMs and subcellular localization of the GCRV encoded proteins were investigated

NS79 exhibited liquid-liquid phase separation (LLPS) characteristics

Liu et al., iScience 27, 110502
August 16, 2024
https://doi.org/10.1016/j.isci.2024.110502

iScience

CellPress
OPEN ACCESS

Article

Biochemical profiling of the protein encoded by grass carp reovirus genotype II

Man Liu,[1,2,3] Chen Xu,[2,3] Yong Zhou,[2] Mingyang Xue,[2] Nan Jiang,[2] Yiqun Li,[2] Zhenyu Huang,[2] Yan Meng,[2] Wenzhi Liu,[2] Xianghui Kong,[1,*] and Yuding Fan[2,4,*]

SUMMARY

In this study, we obtained the whole genome sequence of GCRV-DY197 and investigated the localization, post-translational modifications, and host interactions of the 11 viral proteins encoded by GCRV-DY197 in grass carp ovary (GCO) cells. The whole genome sequence is 24,704 kb and contains 11 segments (S1–S11). Subcellular localization showed that the VP1, VP2, VP3, VP5, VP56, and VP35 proteins were localized in both cytoplasm and nucleus, whereas the NS79, VP4, VP41, VP6, and NS38 proteins were localized in the cytoplasm. The NS79 and NS38 proteins were phosphorylated, and the ubiquitination modification sites were identified in VP41 and NS38. An interaction network containing 9 viral proteins and 140 host proteins was also constructed. These results offer a theoretical basis for an in-depth understanding of the biochemical characteristics and pathogenic mechanism of GCRV-II.

INTRODUCTION

The grass carp (*Ctenopharyngodon idella*) is an important freshwater economic fish in China. According to the China Fishery Statistical Yearbook of 2023, the aquaculture production of grass carp was 5.9 million tons accounting for approximately 18% of total freshwater aquaculture production.[1] In the process of intensive farming, grass carp are threatened by a variety of bacterial and viral diseases, in particular, the hemorrhagic disease caused by the grass carp reovirus (GCRV).[2] Epidemic occurrences of grass carp hemorrhagic disease are an annual phenomenon in numerous Chinese provinces, characterized by mortality rates reaching as high as 85% or even greater, resulting in significant economic losses.[3] GCRV is a double-stranded RNA (dsRNA) virus that belongs to the genus *Aquareovirus* and family *Reoviridae*.[4] GCRV virion has an icosahedral symmetry with a diameter of 60–85 nm. Since the first discovery of GCRV in 1983, more than 40 strains have been isolated and identified, which be divided into three genotypes (GCRV I-III) according to the genomic sequence and epidemiological features.[5,6] GCRV-II is accountable for the significant outbreaks of grass carp hemorrhagic disease in China.[7] However, there is limited information about the pathogenic mechanism of GCRV-II, as GCRV-II was less toxic to the grass carp cell lines and is unable to induce a typical cytopathic effect (CPE) compared to GCRV-I.[8]

The GCRV-II genome contains 11 dsRNA segments, encoding a total of 11 structural and non-structural proteins.[5] The structural proteins VP1, VP3, VP5, VP6, and VP35 make up the double-layered capsid of GCRV-II. Among them, the VP3 protein molecules form the inner core shell of the viral particle.[9] VP5 and VP35 form the outer shell of virus particles in the form of heterodimers.[10] VP1 and VP6 are located between the inner and outer nucleocapsid of the virus particle. VP2 is predicted to be an RNA-dependent RNA polymerase (RdRp), primarily responsible for synthesizing the viral genome's mRNA.[11] VP4 possesses NTPase and RTPase enzyme activities, serving as an important auxiliary factor during viral genome replication.[12,13] The fibrin VP56 encoded by the S7 fragment is involved in virus attachment and viral protein expression.[14] VP41 encoded by the S8 fragment has no homologous protein with other aquatic viruses. Previous studies have shown that VP41 is located in the endoplasmic reticulum of cells and can promote viral RNA synthesis by inhibiting interferon (IFN) expression.[15] Segments S4 and S10 encode non-structural proteins NS79 and NS38, primarily localized in the cytoplasm, forming viral inclusion bodies.[16] VP35 encoded by S11 gene contains zinc-binding motif CxxC-n16-HxC,[17] which is similar to VP7 of GCRV-I and is presumed to be the coat protein of virion.[18]

Studying protein structure, subcellular localization, and virus-host protein-protein interactions (PPIs) can help us better understand the process of virus multiplication and the development of disease.[19,20] Mass spectrometry (MS) has been widely used in protein science, including the identification of the protein sequence and post-translational modification (PTM).[21] Combined with the separation and purification of proteins, MS also is applied to explore PPIs in a range of species.[22–24] For example, affinity purification mass spectrometry (APMS) and co-fractionation coupled with mass spectrometry (CoFrac-MS) are considered ideal techniques for constructing PPI maps.[17,25–27]

[1]Engineering Lab of Henan Province for Aquatic Animal Disease Control, College of Fisheries, Henan Normal University, Xinxiang 453000, China
[2]Yangtze River Fisheries Research Institute, Chinese Academy of Fishery Sciences, Wuhan 430223, China
[3]These authors contributed equally
[4]Lead contact
*Correspondence: xhkong@htu.cm (X.K.), fanyd@yfi.ac.cn (Y.F.)
https://doi.org/10.1016/j.isci.2024.110502

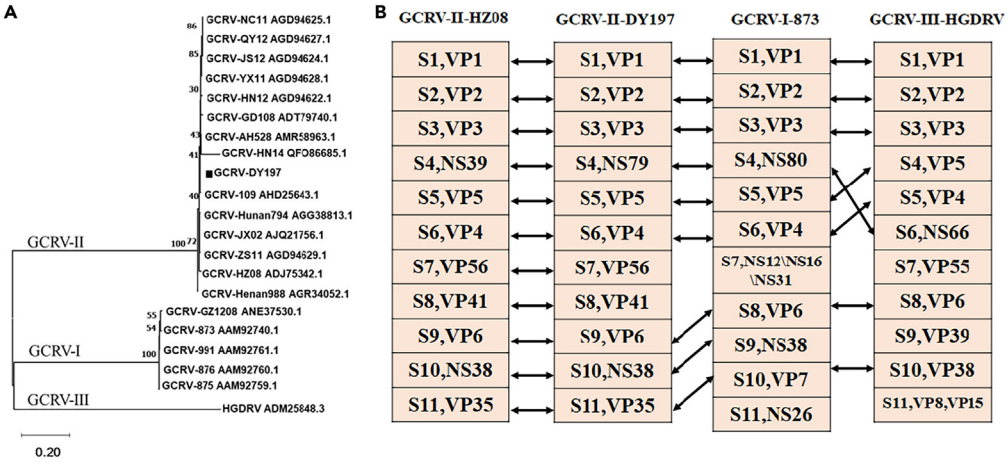

Figure 1. The GCRV-DY197 genome and sequence analysis

(A) Phylogenetic analysis of GCRV-DY197 and other grass carp reovirus strains based on the core protein VP6. The phylogenetic tree was constructed using the neighbor-joining method using 500 bootstrap replicates. The scale bar indicates the evolutionary distance (the average number of amino acid substitutions per site).

(B) The equivalent relationships of predicted proteins in three genotypes of GCRV. Double-headed arrows indicate equivalent proteins.

In this study, we isolated a new strain of GCRV-II, GCRV-DY197, from diseased grass carp and explored the virus proliferation in grass carp liver cell line (L8824) and the liver, spleen, and kidneys. The eleven virus-encoded proteins were amplified and ligated into the pEGFP-N1 vector, and the localization, PTM, and interaction of each protein in GCO cells were elucidated by confocal microscope and APMS. This study offers a more comprehensive understanding of the relationship between GCRV-II and grass carp.

RESULTS

The GCRV-DY197 genome and sequence analysis

The full length of the GCRV-DY197 strain genome is 24,704 kb containing 11 segments (S1–S11), the size of which ranged from 1,027 to 3,928 bp (Table S3), and the accession numbers in GenBank are PP196473–PP196483 https://www.ncbi.nlm.nih.gov/nuccore/PP196473 GCRV-DY197 has more than 95% sequence homology with the GCRV-II-106, 108, 109, and HZ08 strains (Table S4). Based on the amino acid sequence of the VP6, a phylogenetic tree was constructed that can be classified into three genotypes. GCRV-DY197 was closely related to GCRV-II AN528, GD108, HN14, and 109 and apart from GCRV-I and GCRV-III (Figure 1A). Based on the principle of functional similarity of homologous proteins in the *Aquareovirus* family, the correspondence between segments and encoded proteins in the genomes of the three genotypes of GCRV was further clarified (Figure 1B).

GCRV-DY197 showed amino acid mutations in various segments compared to the GCRV-II 106, 108, 109, and HZ08 strains. For example, the S1 segment has two amino acid differences, a mutation of leucine to phenylalanine at position 1,010 and a mutation of isoleucine to threonine at position 1,281. The S3 segment has one amino acid difference, a mutation of glycine to arginine at position 1,230, and three amino acid differences in the S4 segment, a mutation of valine to aspartic acid at position 8, a mutation of serine to glycine at position 132, and a mutation of alanine to serine at position 414. The S6 segment has one amino acid difference, a mutation from glycine to aspartic acid, at position 21. The S8 segment has one amino acid difference, a mutation from proline to serine at position 123 (Figure S2). The number of proteins encoded by the 11 gene segments varies among the three genotyped GCRV strains. Specifically, GCRV-I encodes 13 proteins, GCRV-III encodes 12 proteins, and GCRV-II encodes 11 proteins, with each gene segment in GCRV-II encoding a single protein (Figure 1B). For example, the S7 segment in GCRV-I encodes three non-structural proteins, NS31, NS16, and NS12, of which NS16 is unique to GCRV-I and predicted to be a fusion-associated small transmembrane (FAST) protein involved in host cell-cell fusion.[28] NS12 is a transmembrane protein different from the fusion protein NS16, and its expression alone cannot induce syncytial formation.[29] By contrast, the GCRV-II/GCRV-III S7 segment encodes the fiber protein VP56/VP55, which is involved in viral attachment and expression.[14,30] The GCRV-I S11 segment encodes NS26 that has no homolog in GCRV-II and GCRV-III, which S11 encoded VP35 in GCRV-II predicted to be a coat protein of virion; the function of VP8 and VP15 encoded by S11 in GCRV-III was still unclear.[10]

Proliferative characteristics of the GCRV-DY197

To investigate the virulence and pathogenicity of GCRV-DY197, healthy rare minnows and grass carp were infected with GCRV-DY197, and the clinical features and survival rates were observed. Starting from the third and sixth day's post-viral injection, the rare minnows and grass carp exhibited swimming disorders and sluggish responses. Subsequently, varying degrees of hemorrhagic symptoms manifested on the fish body surface, accompanied by mortality (Figures 2A and S3). Day 6 and 10 after viral injection the mortality rate of rare minnows and grass carp

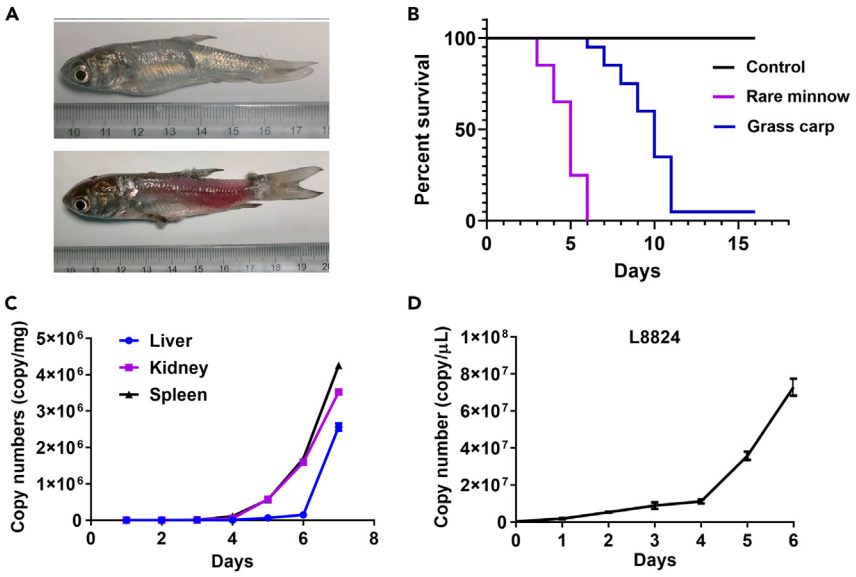

Figure 2. The virulence and proliferative characteristics of GCRV-DY197

(A) The image shows the symptoms of grass carp muscular hemorrhage after GCRV-DY197 infection for 6 days. Top: control; bottom: infection group.

(B) The survival curves of grass carp and rare minnows after GCRV-DY197 infection; $n = 20$.

(C) The viral loads for different days of infection in organs of grass carp.

(D) The changes of the viral loads in L8824 cell line after GCRV-DY197 infection.

were up to 100% and 95%, respectively (Figure 2B). The viral loads were quantified in the liver, spleen, and kidney of grass carp that began growing rapidly 5–6 days post-viral injection, which is consistent with the occurrence time of clinical symptoms (Figure 2C). The GCRV-DY197 proliferation in the L8824 cell line was also investigated growing rapidly four days post-viral infection and up to 7×10^6 copies/μL at 6 days (Figure 2D). Usually, the host's immune systems play an essential role in inhibiting the viral proliferative. We observed that the genes of innate and adaptive immune systems, such as *ifn*, *mx*, *mhc*-I, and *igm*, were upregulated after GCRV-DY197 infection in the spleen of grass carp. The innate immune genes respond faster to viral infection compared to the adaptive immune genes and begin to attenuate at about five days post-infection (Figure 3). These results indicated that the GCRV-DY197 strain can proliferate both *in vivo* and *in vitro* of grass carp and effectively trigger the host's innate and adaptive immune systems.

Characteristics of the GCRV virus-host interaction network

The map of the GCRV virus-host interaction network was built based on the APMS results that comprise 9 virus proteins and 140 host proteins. However, we failed to enrich the VP2-GFP and VP35-GFP proteins as it may be caused by their particular structure or fast turnover rate (Figure 4A). Most host proteins only interacted with one viral protein, whereas parts of host proteins were associated with several viral proteins. For example, the serine/threonine-protein kinase Vrk1 interacts with structural proteins VP5 and VP6 and non-structural proteins VP41 and NS79. Hsp70 was found in the prey of VP1, VP3, and NS38 which may affect the correct folding of viral proteins. Gene ontology (GO) enrichment analysis showed that the 140 host proteins were mainly located at the cellular actin cytoskeleton, nucleolus, and mitochondrial protein-containing complex, which influenced the processes of cellular component morphogenesis, positive regulation of macromolecule biosynthetic process, cell division, and ubiquitin-dependent protein catabolic process (Figure 4B).

Subcellular localization of GCRV-II-encoded proteins in GCO cells

We observed by confocal microscopy the localization of 11 virus-GFP fusion proteins in GCO cells. The VP1, VP2, VP3, VP5, VP56, and VP35 proteins were distributed in both cytoplasm and nucleus, and the content of VP1 and VP2 protein in the cytoplasm seemed to be higher than that in the nucleus—only the VP5 protein was primarily distributed in the nucleus (Figure 5). VP2, VP3, and VP35 were also found in the damaged nucleus, which implied that these proteins may induce apoptosis in GCO cells (Figure 6). The NS79, VP4, VP41, VP6, and NS38 proteins are all localized in the cytoplasm, but the aggregation states of each protein are different (Figure 5). The NS79 was self-aggregated and scattered in the cytoplasm, which displayed characteristics of liquid-liquid phase separation (LLPS), and NS79-GFP fluorescence was rapidly recovered ~40 s after photobleaching (Figure 7A). VP4, VP41, VP6, and NS38 also presented a certain degree of aggregation but tended to be around the nucleus (Figure 5). It has been reported that NS38 can interact with NS79 and be involved in the formation of viral inclusion bodies (VIBs),[31,32] but the fluorescence of NS38-GFP was not recovered after bleaching, so did not display characteristics of LLPS (Figure 7B). These results revealed the distribution of 11 GCRV-DY197 encoded proteins in GCO cells.

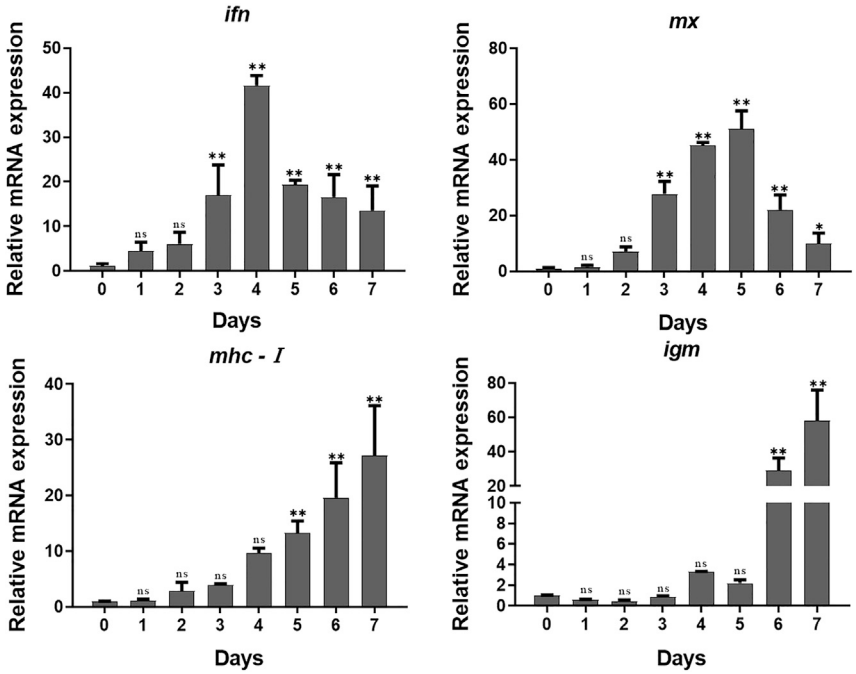

Figure 3. The transcriptional levels of grass carp immune genes

qPCR results show the relative transcript levels of *ifn*, *mx*, *mhc*-I, and *igm* in grass carp after GCRV-DY197 infection. The relative transcription levels for each gene are normalized to that of β-actin. ** $p < 0.01$.

PTMs of GCRV-II encoded proteins

PTMs of proteins, including phosphorylation, ubiquitination, and acetylation, influence protein structure and functions. Previous studies have indicated that both viral and host proteins undergo various modifications during viral infection.[33] We identified phosphorylation modifications at Ser655 and Ser72 residues on the NS79 and NS38 proteins, respectively (Figure 8A). Ubiquitination modifications at the Lys189 residue on both the VP41 and NS38 proteins were observed (Figure 8B). These findings underscore the pivotal role of PTMs in maintaining viral protein normal functions and metabolic rates during viral infection.

DISCUSSION

The GCRV-II is one of the primary pathogens threatening grass carp aquaculture.[34] Multiple strains of GCRV-II have been isolated and sequenced across various regions in China.[35,36] Typically, these strains are categorized into high and low pathogenicity. In this study, we isolated a strain of GCRV-II from Sichuan province that exhibits strong lethality toward both grass carp and rare minnows. The complete sequencing of its genome was achieved. Additionally, by investigating the *in situ* expression of viral-encoded proteins, we observed the localization, modifications, and interactions of these proteins within the cell. This research provides data support for a comprehensive understanding of the functional roles of GCRV-encoded proteins and their pathogenic mechanisms.

Phosphorylation regulation may play a crucial role in the formation of VIBs. VIB formation is a pivotal process during the intracellular proliferation of reovirus within cells, where the non-structural protein NS79 plays a significant role in recruiting viral proteins and nucleic acids, facilitating VIB formation.[37] The NS79 protein exhibits self-aggregation, dispersing across various regions of the cytoplasm and displaying characteristics of LLPS. Previous research indicates that the aggregation of the NS79 protein relies on interactions among its C-terminal regions (335–724 AA).[38] Loss of this region diminishes the self-aggregation ability of NS79, possibly due to the presence of coiled-coil structural domains mediating interactions between NS79 proteins. In this study, we identified phosphorylation on serine 655 of the NS79 protein. Given its proximity to the coiled-coil domain, this phosphorylation might induce structural alterations, thereby modulating VIB formation. Simultaneously, the TBK1 protein mediates the NS79 protein phosphorylation, but the exact phosphorylation site is unknown.[32,39] Additionally, APMS results show that the VrK1 protein interacts with NS79, but this still needs to be further explored. Another participant in VIB formation, the NS38 protein, also exhibits phosphorylation modifications. NS38 is primarily recruited by the NS79 protein, forming the framework of cytoplasmic VIBs.[40] Deletion of NS38 impacts NS79 protein expression and the proliferation of the virus.[16] However, further validation is needed to determine whether phosphorylation of NS38 can affect the expression and function of the NS79 protein.

The ubiquitin-mediated protein degradation pathway might serve as a significant regulatory mechanism in the host response to viral infections.[41,42] Previous quantitative proteomics studies have revealed a significant upregulation of proteins associated with the ubiquitin-proteasome pathway within the host following GCRV infection.[43] This pathway serves the dual purpose of clearing damaged organelles or

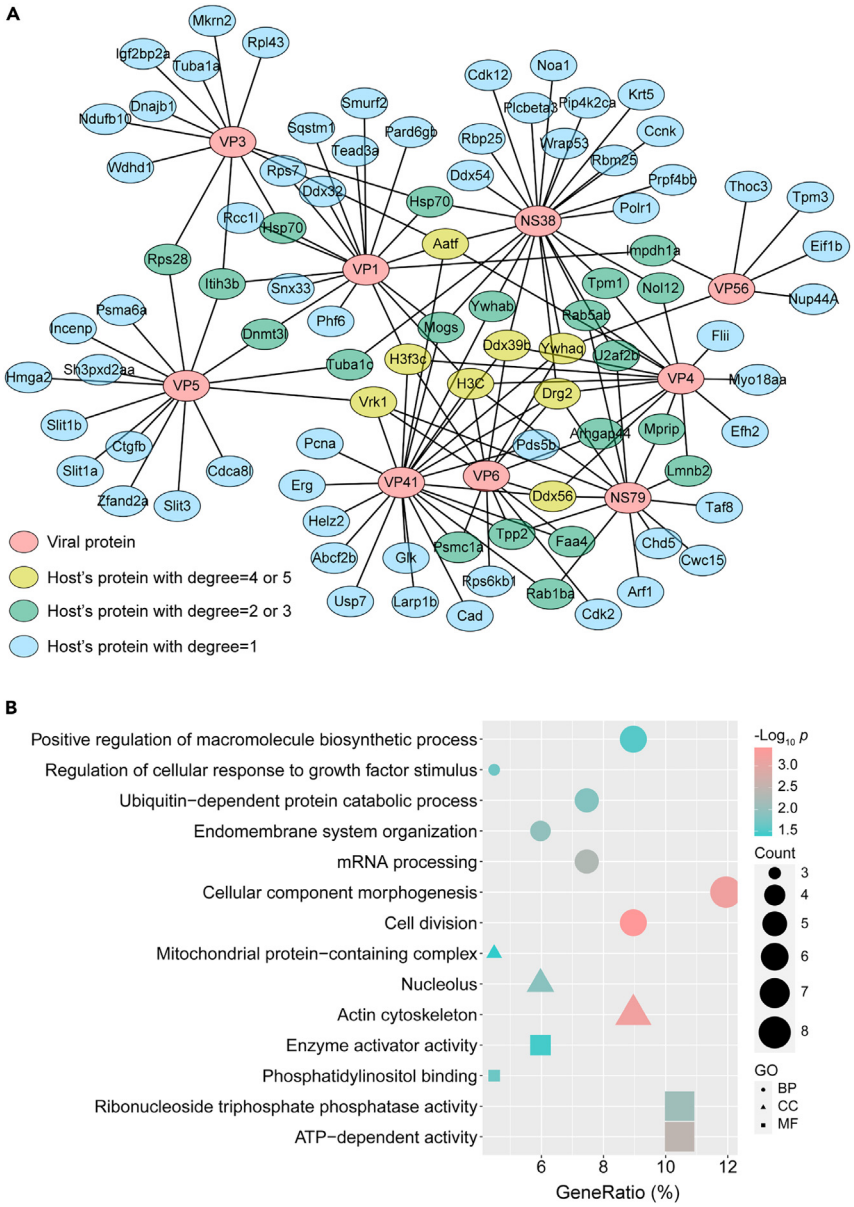

Figure 4. Characteristics of GCRV virus-host interaction network

(A) The map of the virus-host interaction network. The interaction partners of viral proteins were determined by the APMS experiment and SAINT software with a score ≥0.9 and FoldChange ≥20. Host proteins with different degrees are marked with different colors. The network was constructed by Cytoscape software.
(B) GO analysis of 140 interaction partners of 9 viral proteins in GCO cells.

proteins due to viral infection and degrading the viral proteins themselves.[44] In this study, the observation of ubiquitination modifications on VP41 and NS38 proteins reaffirms that viral proteins can indeed undergo host-mediated degradation through the ubiquitination pathway. Both VP41 and NS38 proteins localize within cellular regions such as the endoplasmic reticulum and play crucial regulatory roles in viral proliferation and immune evasion.[15] Both VP41 and NS38 have been reported to inhibit the host's antiviral effect mediated by MAVS.[15] Additionally, VP41 protein interacts with proteins, such as TBK, MAVS, and MITA, suppressing interferon production in host cells, and aiding the virus in immune evasion.[45] In antiviral immune responses, the ubiquitin-proteasome pathway is considered an important way to inhibit viral proliferation.[46] The degradation of viral proteins is also linked to the activation of the host's adaptive immune system.[47] Typically, the peptides from the degraded viral protein can bind with major histocompatibility complex (MHC) molecules within the cell and transfer through the endoplasmic reticulum and Golgi apparatus to the cell membrane, ultimately presenting to lymphocytes, activating the host's adaptive immune response.[48] We believed that the peptides, degraded from VP41 and NS38 proteins through the ubiquitin-proteasome pathway, can quickly

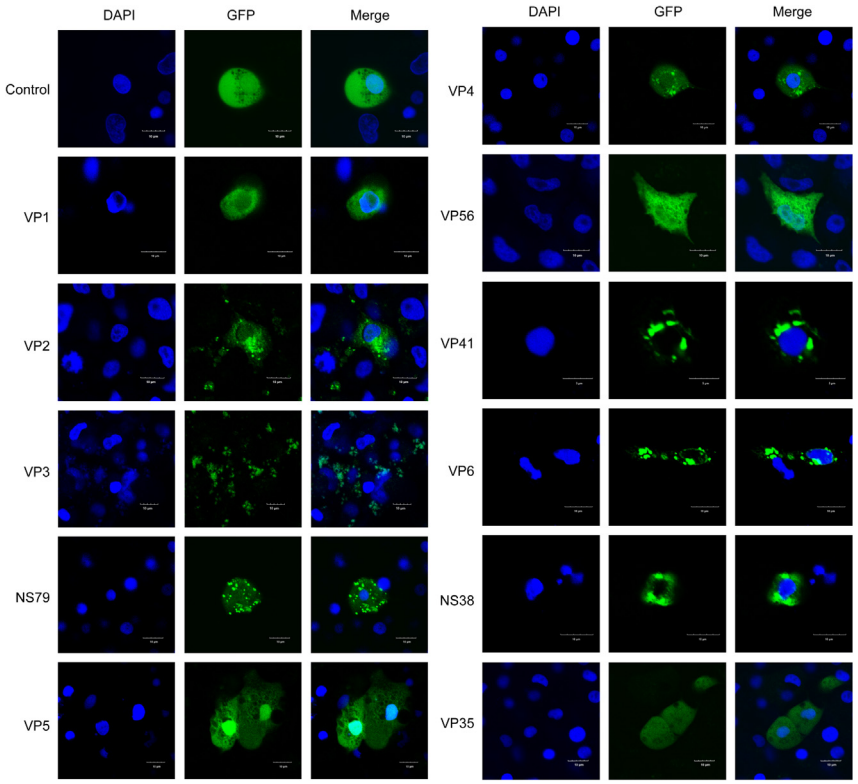

Figure 5. Subcellular localization of viral proteins in GCO cells

The GCO cells that expressed with different viral proteins or GFP were fixed and stained with DAPI. The samples were examined using confocal microscopy equipped with a 40× objective lens.

bind to MHC molecules that are localized at the endoplasmic reticulum and then transfer to the cell membrane. Hence, VP41 and NS38 might exhibit strong immunogenicity, potentially serving as targets in future antiviral drug development.

All animal experiments were approved by the Animal Experimental Ethical Inspection of Laboratory Animal Center, Yangtze River Fisheries Research Institute, Chinese Academy of Fishery Sciences.

Limitations of the study

A virus-host protein interaction network has been constructed in a grass carp cell line; however, further functional validation of specific protein complexes is still required.

STAR★METHODS

Detailed methods are provided in the online version of this paper and include the following:

- KEY RESOURCES TABLE
- RESOURCE AVAILABILITY
  - Lead contact
  - Materials availability
  - Data and code availability
- EXPERIMENTAL MODEL AND STUDY PARTICIPANT DETAILS
  - Viruses
  - Fish
  - Cells
- METHOD DETAILS
  - Whole genome sequencing and analysis
  - Regression infection experiment
  - GCRV-DY197 proliferation *in vitro* and *in vivo*

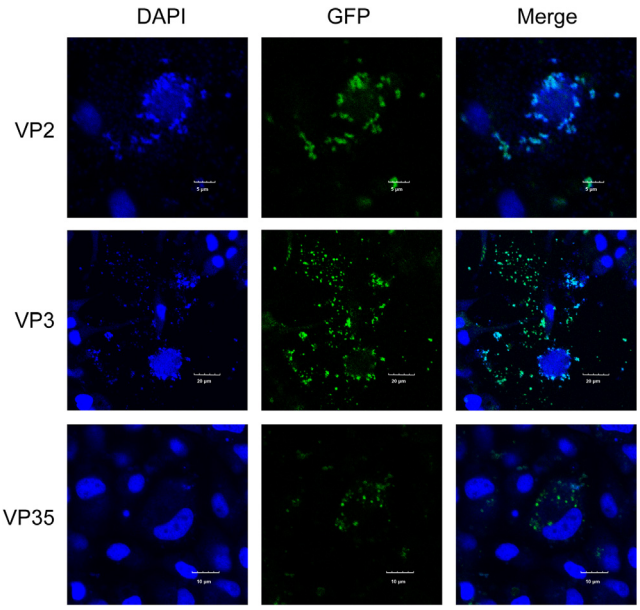

Figure 6. Subcellular localization of VP2, VP3, and VP35 in the damaged nucleus of GCO cells

The GCO cells that expressed with VP2-GFP, VP3-GFP, and VP35-GFP were fixed and stained with DAPI. The samples were examined using confocal microscopy equipped with a 40× objective lens.

- Real-time quantitative PCR
- Plasmid construction and transfection
- Subcellular localization
- Protein extraction
- Affinity purification mass spectrometry

- QUANTIFICATION AND STATISTICAL ANALYSIS

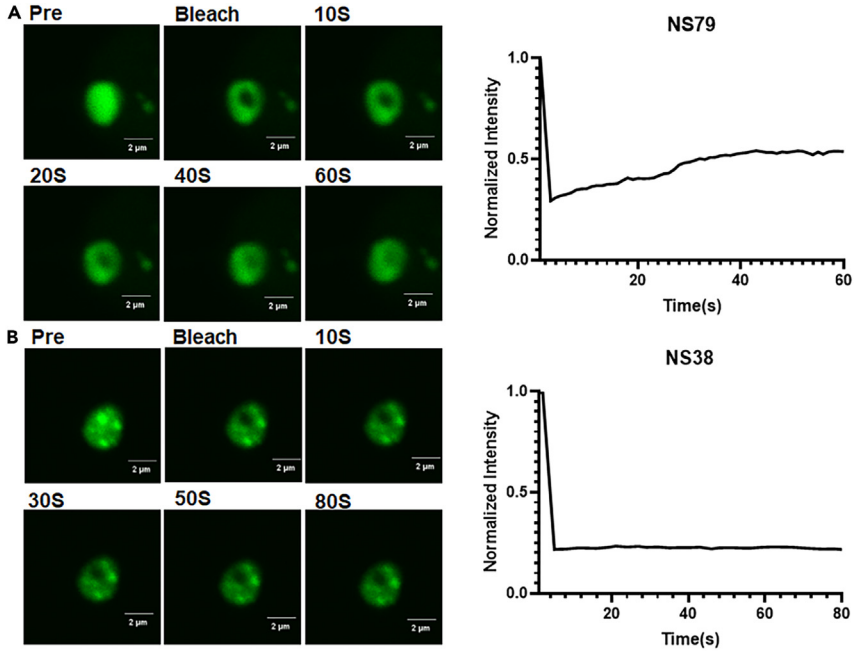

Figure 7. Fluorescence recovery after photo bleaching (FRAP)

Time-lapse images and fluorescent quantitation of NS79-GFP (A) and NS38-GFP (B).

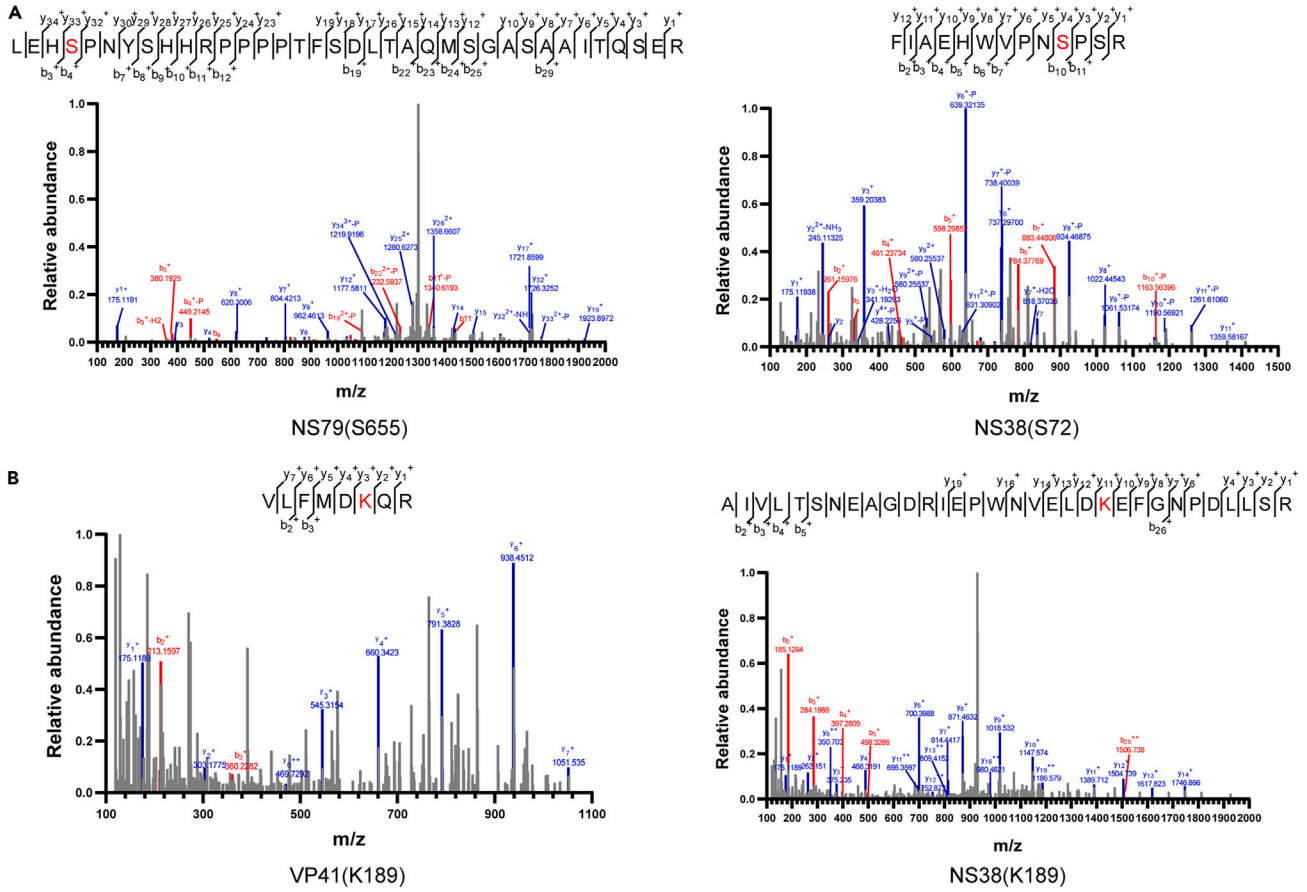

Figure 8. MS/MS spectrum of identified peptides

(A) MS/MS spectrum of phosphorylated peptides in the NS79 and NS38 proteins.

(B) MS/MS spectrum of ubiquitinated peptides in the VP41 and NS38 proteins.

SUPPLEMENTAL INFORMATION

Supplemental information can be found online at https://doi.org/10.1016/j.isci.2024.110502.

ACKNOWLEDGMENTS

We are grateful to all study participants for their contributions.

Funding: This work was sponsored by the Key Program of Natural Science Foundation of Henan Province [grant number 232300421113]; the National Natural Science Foundation of China [grant number 31772894]; the Central Public-interest Scientific Institution Basal Research Fund, Chinese Academy of Fishery Sciences (CAFS) [grant number 2023TD46]; and the Earmarked Fund for China Agriculture Research System [grant number CARS-45].

AUTHOR CONTRIBUTIONS

Conceptualization, M.L., C.X., X.H.K., and Y.D.F., methodology, M.L., C.X., M.Y.X., N.J., Y.M., Y.Q.L., and W.Z.L.; validation, Z.Y.H., W.Z.L., Y.Z., and M.Y.X., formal analysis, M.L. and C.X.; investigation, M.L., M.X., and Y.D.F.; data curation, C.X. and Y.D.F.; writing – original draft preparation, M.L. and C.X.; writing – review and editing, C.X., X.H.K., and Y.D.F.; supervision, C.X. and Y.D.F.; project administration, C.X. and X.H.K.; funding acquisition, N.J. and Y.D.F. All authors have read and agreed to the published version of the manuscript.

DECLARATION OF INTERESTS

The authors declare no competing interests.

Received: February 6, 2024
Revised: April 21, 2024
Accepted: July 10, 2024
Published: July 20, 2024

REFERENCES

1. Tu, C., Yang, S., Yang, M., Liu, L., Tao, J., Zhang, L., Huang, X., Tian, Y., Li, N., Lin, L., and Qin, Z. (2024). Mechanisms of Persistent Hemolysis-Induced middle kidney Injury in grass carp (*Ctenopharyngodon idella*). Fish Shellfish Immunol. *150*, 109603. https://doi.org/10.1016/j.fsi.2024.109603.
2. Rao, Y., and Su, J. (2015). Insights into the Antiviral Immunity against Grass Carp (*Ctenopharyngodon idella*) Reovirus (GCRV) in Grass Carp. J. Immunol. Res. *2015*, 670437. https://doi.org/10.1155/2015/670437.
3. Aymara, A.C.R., Rockemann, D.D., and Samal, S.K. (1999). Identification of grass carp haemorrhage virus as a new genogroup of aquareovirus. J. Gen. Virol. *80*, 2399–2402. https://doi.org/10.1099/0022-1317-80-9-2399.
4. Cheng, L., Fang, Q., Shah, S., Atanasov, I.C., and Zhou, Z.H. (2008). Subnanometer-Resolution Structures of the Grass Carp Reovirus Core and Virion. J. Mol. Biol. *382*, 213–222. https://doi.org/10.1016/j.jmb.2008.06.075.
5. Wang, Q., Zeng, W., Liu, C., Zhang, C., Wang, Y., Shi, C., and Wu, S. (2012). Complete Genome Sequence of a Reovirus Isolated from Grass Carp, Indicating Different Genotypes of GCRV in China. J. Virol. *86*, 12466. https://doi.org/10.1128/jvi.02333-12.
6. Zhang, K., Liu, W., Li, Y., Zhou, Y., Meng, Y., Zeng, L., Vakharia, V.N., and Fan, Y. (2021). Isolation, Identification, and Genomic Analysis of a Novel Reovirus from Healthy Grass Carp and Its Dynamic Proliferation In Vitro and In Vivo. Viruses *13*, 690. https://doi.org/10.3390/v13040690.
7. Jiang, L., Liu, A.q., Zhang, C., Zhang, Y.A., and Tu, J. (2022). Hsp90 Regulates GCRV-II Proliferation by Interacting with VP35 as Its Receptor and Chaperone. J. Virol. *96*, e0117522. https://doi.org/10.1128/jvi.01175-22.
8. Tang, Y., Zeng, W., Wang, Y., Wang, Q., Yin, J., Li, Y., Wang, C., Bergmann, S.M., Gao, C., and Hu, H. (2020). Comparison of the blood parameters and histopathology between grass carp infected with a virulent and avirulent isolates of genotype II grass carp reovirus. Microb. Pathog. *139*, 103859. https://doi.org/10.1016/j.micpath.2019.103859.
9. Martella, V., Ciarlet, M., Pratelli, A., Arista, S., Terio, V., Elia, G., Cavalli, A., Gentile, M., Decaro, N., Greco, G., et al. (2003). Molecular Analysis of the VP7, VP4, VP6, NSP4, and NSP5/6 Genes of a Buffalo Rotavirus Strain: Identification of the Rare P[3] Rhesus Rotavirus-Like VP4 Gene Allele. J. Clin. Microbiol. *41*, 5665–5675. https://doi.org/10.1128/jcm.41.12.5665-5675.2003.
10. Gao, Y., Pei, C., Sun, X., Zhang, C., Li, L., and Kong, X. (2018). Novel subunit vaccine based on grass carp reovirus VP35 protein provides protective immunity against grass carp hemorrhagic disease. Fish Shellfish Immunol. *75*, 91–98. https://doi.org/10.1016/j.fsi.2018.01.050.
11. Pan, M., Alvarez-Cabrera, A.L., Kang, J.S., Wang, L., Fan, C., and Zhou, Z.H. (2021). Asymmetric reconstruction of mammalian reovirus reveals interactions among RNA, transcriptional factor μ2 and capsid proteins. Nat. Commun. *12*, 4176. https://doi.org/10.1038/s41467-021-24455-4.
12. Wang, X., Zhang, F., Su, R., Li, X., Chen, W., Chen, Q., Yang, T., Wang, J., Liu, H., Fang, Q., and Cheng, L. (2018). Structure of RNA polymerase complex and genome within a dsRNA virus provides insights into the mechanisms of transcription and assembly. Proc. Natl. Acad. Sci. USA *115*, 7344–7349. https://doi.org/10.1073/pnas.1803885115.
13. Yan, L., Guo, H., Sun, X., Shao, L., and Fang, Q. (2012). Characterization of grass carp reovirus minor core protein VP4. Virol. J. *9*, 89. https://doi.org/10.1186/1743-422X-9-89.
14. Pei, C., Gao, Y., Sun, X., Li, L., and Kong, X. (2019). A developed subunit vaccine based on fiber protein VP56 of grass carp reovirus providing immune protection against grass carp hemorrhagic disease. Fish Shellfish Immunol. *90*, 12–19. https://doi.org/10.1016/j.fsi.2019.04.055.
15. Lu, L.F., Li, S., Wang, Z.X., Du, S.Q., Chen, D.D., Nie, P., Zhang, Y.A., and Lyles, D.S. (2017). Grass Carp Reovirus VP41 Targets Fish MITA To Abrogate the Interferon Response. J. Virol. *91*, e00390-17. https://doi.org/10.1128/jvi.00390-17.
16. Zhang, J., Guo, H., Zhang, F., Chen, Q., Chang, M., and Fang, Q. (2019). NS38 is required for aquareovirus replication via interaction with viral core proteins and host eIF3A. Virology *529*, 216–225. https://doi.org/10.1016/j.virol.2019.01.029.
17. Deen, A.J., Adinolfi, S., Härkönen, J., Patinen, T., Liu, X., Laitinen, T., Takabe, P., Kainulainen, K., Pasonen-Seppänen, S., Gawriyski, L.M., et al. (2024). Oncogenic KEAP1 mutations activate TRAF2-NFκB signaling to prevent apoptosis in lung cancer cells. Redox Biol. *69*, 103031. https://doi.org/10.1016/j.redox.2024.103031.
18. Lu, L.F., Zhang, C., Li, Z.C., Zhou, X.Y., Jiang, J.Y., Chen, D., Zhang, Y.A., and Li, S. (2021). Grass Carp Reovirus VP35 Degrades MAVS Through the Autophagy Pathway to Inhibit Fish Interferon Production. Front. Immunol. *12*, 613145. https://doi.org/10.3389/fimmu.2021.613145.
19. Ding, K., Nguyen, L., and Zhou, Z.H. (2018). In Situ Structures of the Polymerase Complex and RNA Genome Show How Aquareovirus Transcription Machineries Respond to Uncoating. J. Virol. *92*, e00774-18. https://doi.org/10.1128/jvi.00774-00718.
20. Zhang, J., Li, P., Lu, R., Ouyang, S., and Chang, M.X. (2022). Structural and functional analysis of the small GTPase ARF1 reveals a pivotal role of its GTP-binding domain in controlling of the generation of viral inclusion bodies and replication of grass carp reovirus. Front. Immunol. *13*, 956587. https://doi.org/10.3389/fimmu.2022.956587.
21. Neagu, A.N., Jayathirtha, M., Baxter, E., Donnelly, M., Petre, B.A., and Darie, C.C. (2022). Applications of Tandem Mass Spectrometry (MS/MS) in Protein Analysis for Biomedical Research. Molecules *27*, 2411. https://doi.org/10.3390/molecules27082411.
22. Zhang, C., Lu, L.F., Li, Z.C., Zhou, X.Y., Zhou, Y., Chen, D.D., Li, S., and Zhang, Y.A. (2020). Grass carp reovirus VP56 represses interferon production by degrading phosphorylated IRF7. Fish Shellfish Immunol. *99*, 99–106. https://doi.org/10.1016/j.fsi.2020.02.004.
23. Qin, X., Li, X., Chen, L., Gao, T., Luo, J., Guo, L., Mollah, S., Zhang, Z., Zhou, Y., and Chen, H.-X. (2024). Characterization of Adeno-Associated Virus Capsid Proteins by Microflow Liquid Chromatography Coupled with Mass Spectrometry. Appl. Biochem. Biotechnol. *196*, 1623–1635. https://doi.org/10.1007/s12010-023-04656-x.
24. Le, T.D., Suttikhana, I., and Ashaolu, T.J. (2023). State of the art on the separation and purification of proteins by magnetic nanoparticles. J. Nanobiotechnol. *21*, 363. https://doi.org/10.1186/s12951-023-02123-7.
25. Wang, X.N., Sim, B.R., Chen, H., Zheng, Y.X., Xue, J.B., Wang, L., Kong, W.S., Zhou, K., Guo, S.J., Hou, J.L., et al. (2022). Identification of sitagliptin binding proteins by affinity purification mass spectrometry. Acta Biochim. Biophys. Sin. *54*, 1453–1463. https://doi.org/10.3724/abbs.2022142.
26. Havugimana, P.C., Goel, R.K., Phanse, S., Youssef, A., Padhorny, D., Kotelnikov, S., Kozakov, D., and Emili, A. (2022). Scalable multiplex co-fractionation/mass spectrometry platform for accelerated protein interactome discovery. Nat. Commun. *13*, 4043. https://doi.org/10.1038/s41467-022-31809-z.
27. O'Reilly, F.J., Graziadei, A., Forbrig, C., Bremenkamp, R., Charles, K., Lenz, S., Elfmann, C., Fischer, L., Stülke, J., and Rappsilber, J. (2023). Protein complexes in cells by AI-assisted structural proteomics. Mol. Syst. Biol. *19*, e11544. https://doi.org/10.15252/msb.202311544.
28. Guo, H., Chen, Q., Yan, L., Zhang, J., Yan, S., Zhang, F., and Fang, Q. (2015). Identification of a functional motif in the AqRV NS26 protein required for enhancing the fusogenic activity of FAST protein NS16. J. Gen. Virol. *96*, 1080–1085. https://doi.org/10.1099/vir.0.000057.
29. Yu, F., Wang, L., Li, W., and Lu, L. (2019). Identification of a novel membrane-associated protein from the S7 segment of grass carp reovirus. J. Gen. Virol. *100*, 369–379. https://doi.org/10.1099/jgv.0.001223.
30. Tian, Y., Jiao, Z., Dong, J., Sun, C., Jiang, X., and Ye, X. (2017). Grass carp reovirus-GD108 fiber protein is involved in cell attachment. Virus Gene. *53*, 613–622. https://doi.org/10.1007/s11262-017-1467-6.
31. Li, P.W., Zhang, J., and Chang, M.X. (2023). Structure, function and immune evasion strategies of aquareoviruses, with focus on grass carp reovirus. Rev. Aquacult. *16*, 410–432. https://doi.org/10.1111/raq.12844.

32. Lu, L.F., Li, Z.C., Zhang, C., Zhou, X.Y., Zhou, Y., Jiang, J.Y., Chen, D.D., Li, S., and Zhang, Y.-A. (2020). Grass Carp Reovirus (GCRV) Giving Its All to Suppress IFN Production by Countering MAVS Signaling Transduction. Front. Immunol. *11*, 545302. https://doi.org/10.3389/fimmu.2020.545302.
33. Xu, C., Li, Y., Xiao, Z., Yang, J., Xue, M., Jiang, N., Meng, Y., Liu, W., Fan, Y., and Zhou, Y. (2022). Proteomic and Phosphoproteomic Analyses Reveal Gibel Carp Responses to Cyprinid Herpesvirus 2 Infection. J. Proteome Res. *21*, 1961–1973. https://doi.org/10.1021/acs.jproteome.2c00253.
34. Wu, M., Li, H., Chen, X., Jiang, Y., and Jiang, W. (2020). Studies on the clinical symptoms, virus distribution, and mRNA expression of several antiviral immunity-related genes in grass carp after infection with genotype II grass carp reovirus. Arch. Virol. *165*, 1599–1609. https://doi.org/10.1007/s00705-020-04654-y.
35. Brown, E.G., Nibert, M.L., and Duncan, R. (2013). Bioinformatics of Recent Aqua and Orthoreovirus Isolates from Fish: Evolutionary Gain or Loss of FAST and Fiber Proteins and Taxonomic Implications. PLoS One *8*, e68607. https://doi.org/10.1371/journal.pone.0068607.
36. He, L., Zhang, A., Pei, Y., Chu, P., Li, Y., Huang, R., Liao, L., Zhu, Z., and Wang, Y. (2017). Differences in responses of grass carp to different types of grass carp reovirus (GCRV) and the mechanism of hemorrhage revealed by transcriptome sequencing. BMC Genom. *18*, 452. https://doi.org/10.1186/s12864-017-3824-1.
37. Shao, L., Guo, H., Yan, L.M., Liu, H., Fang, Q., and Fang, Q. (2013). Aquareovirus NS80 Recruits Viral Proteins to Its Inclusions, and Its C-Terminal Domain Is the Primary Driving Force for Viral Inclusion Formation. PLoS One *8*, e55334. https://doi.org/10.1371/journal.pone.0055334.
38. Miller, C.L., Broering, T.J., Parker, J.S.L., Arnold, M.M., and Nibert, M.L. (2003). Reovirus σNS Protein Localizes to Inclusions through an Association Requiring the μNS Amino Terminus. J. Virol. *77*, 4566–4576. https://doi.org/10.1128/jvi.77.8.4566-4576.2003.
39. Zhang, J., Man Wu, X., Fang, Q., Bi, Y.H., Nie, P., and Chang, M.X. (2022). Grass Carp Reovirus Nonstructural Proteins Avoid Host Antiviral Immune Response by Targeting the RLR Signaling Pathway. J. Immunol. *208*, 707–719. https://doi.org/10.4049/jimmunol.2100723.
40. Yan, L., Zhang, J., Guo, H., Yan, S., Chen, Q., Zhang, F., Fang, Q., and Fang, Q. (2015). Aquareovirus NS80 Initiates Efficient Viral Replication by Retaining Core Proteins within Replication-Associated Viral Inclusion Bodies. PLoS One *10*, e0126127. https://doi.org/10.1371/journal.pone.0126127.
41. Oshiumi, H., Matsumoto, M., and Seya, T. (2012). Ubiquitin-mediated modulation of the cytoplasmic viral RNA sensor RIG-I. J. Biochem. *151*, 5–11. https://doi.org/10.1093/jb/mvr111.
42. Su, H.,L.Z., Yang, C., Zhang, Y., and Su, J. (2021). Grass carp reovirus VP56 allies VP4, recruits, blocks, and degrades RIG-I to more effectively attenuate IFN responses and facilitate viral evasion. Microbiol. Spectr. *9*, e0100021. https://doi.org/10.1128/Spectrum.
43. Xu, C., Yang, J., Cao, J., Jiang, N., Zhou, Y., Zeng, L., Zhong, Q., and Fan, Y. (2022). The quantitative proteomic analysis of rare minnow, Gobiocypris rarus, infected with virulent and attenuated isolates of grass carp reovirus genotype II. Fish Shellfish Immunol. *123*, 142–151. https://doi.org/10.1016/j.fsi.2022.02.037.
44. Oshiumi, H. (2020). Recent Advances and Contradictions in the Study of the Individual Roles of Ubiquitin Ligases That Regulate RIG-I-Like Receptor-Mediated Antiviral Innate Immune Responses. Front. Immunol. *11*, 1296. https://doi.org/10.3389/fimmu.2020.01296.
45. Xu, X., Li, M., Deng, Z., Jiang, Z., Li, D., Wang, S., and Hu, C. (2021). cGASa and cGASb from grass carp (*Ctenopharyngodon idellus*) play opposite roles in mediating type I interferon response. Dev. Comp. Immunol. *125*, 104233. https://doi.org/10.1016/j.dci.2021.104233.
46. Zhang, J., and Chang, M.X. (2023). TBK1 Isoform Inhibits Grass Carp Reovirus Infection by Targeting the Degradation of Viral Nonstructural Proteins NS80 and NS38. J. Immunol. *210*, 191–203. https://doi.org/10.4049/jimmunol.2200471.
47. Zhao, X., Dan, C., Gong, X.Y., Li, Y.L., Qu, Z.L., Sun, H.Y., An, L.L., Guo, W.H., Gui, J.F., and Zhang, Y.B. (2022). Zebrafish MARCH8 downregulates fish IFN response by targeting MITA and TBK1 for protein degradation. Dev. Comp. Immunol. *135*, 104485. https://doi.org/10.1016/j.dci.2022.104485.
48. Buzuk, L., and Hellerschmied, D. (2023). Ubiquitin-mediated degradation at the Golgi apparatus. Front. Mol. Biosci. *10*, 1197921. https://doi.org/10.3389/fmolb.2023.1197921.
49. Ma, J., Xu, C., Zhou, Y., Jiang, N., Xue, M., Cao, J., Li, S., and Fan, Y. (2023). Metabolomics in rare minnow (*Gobiocypris rarus*) after infection by attenuated and virulent grass carp reovirus genotype II. Fish Shellfish Immunol. *138*, 108840. https://doi.org/10.1016/j.fsi.2023.108840.
50. Dai, Y., Li, Y., Hu, X., Jiang, N., Liu, W., Meng, Y., Zhou, Y., Xu, C., Xue, M., and Fan, Y. (2023). Nonstructural protein NS17 of grass carp reovirus Honghu strain promotes virus infection by mediating cell-cell fusion and apoptosis. Virus Res. *334*, 199150. https://doi.org/10.1016/j.virusres.2023.199150.
51. Liu, L., Gong, Y.X., Liu, G.L., Zhu, B., and Wang, G.X. (2016). Protective immunity of grass carp immunized with DNA vaccine against Aeromonas hydrophila by using carbon nanotubes as a carrier molecule. Fish Shellfish Immunol. *55*, 516–522. https://doi.org/10.1016/j.fsi.2016.06.026.

STAR★METHODS

KEY RESOURCES TABLE

REAGENT or RESOURCE	SOURCE	IDENTIFIER
Antibodies		
Rabbit polyclonal to GFP	abcam	Cat#ab290; RRID : AB_722150
Bacterial and virus strains		
Grass Carp Reovirus (GCRV), type II, strain GCRV-DY197	Isolated and preserved in our laboratory	N/A
Chemicals, peptides, and recombinant proteins		
SMARTer RACE 5′/3′ Kit	Clontech	Cat#634860
TRIzol reagents	Invitrogen	
EasyScript®One-Step gDNA Removal and cDNA Synthesis SuperMix Kit	TransGen Biotech	Cat#AE341-02
TB Green®Premix Ex Taq™ II	TaKaRa	Cat#CN830A
Endotoxin-free kit	Omega	Cat#D6950-02
DL-Dithiothreitol (DTT)	Sigma	Cat#3483-12-3
Iodoacetamide (IAM)	Sigma	Cat#DI6125
Fetal Bovine Serum (FBS)	Yeasen	Cat#40130ES76
Medium199	HyClone	Cat#SH30253.01
PBS	HyClone	Cat#SH30256.01
Xfect™ Transfection Reagent	TaKaRa	Cat#631318
4% paraformaldehyde	Biosharp	Cat#BL539A
DAPI	Biosharp	Cat#BL105A
Protein A Magnetic Beads	GenScript	Cat# L00695
Experimental models: Cell lines		
Healthy rare minnows	From the Institute of Hydrobiology, Chinese Academy of Sciences (Wuhan, China)	N/A
Healthy grass carp	From the Hubei grass carp farm	N/A
GCO cell (Grass carp ovary cell line)	Gift from QiYa Zhang (the Institute of Hydrobiology, Chinese Academy of Sciences)	N/A
L8824 cell (Grass carp Grass carp hepatocytes)	Center for the Preservation of Chinese Typical Cultures, Wuhan University	N/A
Oligonucleotides		
See Table S1	Huayu Gene	N/A
See Table S2	Huayu Gene	N/A
Recombinant DNA		
Plasmid VP1-GFP	This paper	PP196473
Plasmid VP2-GFP	This paper	PP196474
Plasmid VP3-GFP	This paper	PP196475
Plasmid NS79-GFP	This paper	PP196476
Plasmid VP5-GFP	This paper	PP196477
Plasmid VP4-GFP	This paper	PP196478
Plasmid VP56-GFP	This paper	PP196479
Plasmid VP41-GFP	This paper	PP196480
Plasmid VP6-GFP	This paper	PP196481

(*Continued on next page*)

Continued

REAGENT or RESOURCE	SOURCE	IDENTIFIER
Plasmid NS38-GFP	This paper	PP196482
Plasmid VP35-GFP	This paper	PP196483
Software and algorithms		
SEQMAN	DNASTAR 5.0	N/A
Simple Modular Architecture Research Tool	SMART	N/A
Proteome Discoverer 2.4	Thermo Fisher Scientific	N/A
SAINT	https://sourceforge.net/projects/saint-apms/files/	N/A
Other		
FV3000	Olympus	N/A
Roter-Gene Q	Qiagen	N/A
ChemiDox XRS	Bio-Rad	N/A
Q-Exactive Plus	Thermo Fisher Scientific	N/A

RESOURCE AVAILABILITY

Lead contact

Further information and requests for resources and reagents should be directed to and will be fulfilled by the lead contact, YuDing Fan (fanyd@yfi.ac.cn).

Materials availability

This study did not generate unique reagents.

Data and code availability

- All data reported in this paper will be shared by the lead contact upon reasonable request.
- This paper does not report original code.
- Any additional information required to reanalyze the data reported in this paper is available from the lead contact upon request.

EXPERIMENTAL MODEL AND STUDY PARTICIPANT DETAILS

Viruses

GCRV-DY197 strain was obtained from diseased grass carp collected from a farm in Deyang, Sichuan Province.[49] The liver, spleen, and kidney of diseased grass carp were extracted and homogenized with PBS five times followed by freeze-thawing at −80°C three times. The tissue homogenate containing GCRV was collected after being centrifuged at 3,000 × g for 30 min and filtered through 0.45 μm and 0.22 μm filters (Millipore, USA).

Fish

Healthy rare minnows, measuring 4 ± 0.5 cm in length, were acquired from the Institute of Hydrobiology, Chinese Academy of Sciences (Wuhan, China). Healthy grass carp with lengths of 10.0 ± 0.5 cm were purchased from the Hubei grass carp farm. All the experimental fish were shown to be GCRV-negative according to the national standards and were kept in the laboratory for two weeks before the virus challenge. All the experimental procedure were approved by the Yangtze River Fisheries Research Institute's Animal Experimental Ethical Committee.

Cells

Grass carp ovary (GCO) cells and grass carp liver cells were cultured in medium (M199) (Gibco) containing 10% fetal bovine serum (FBS) (Gibco) at 28°C.

METHOD DETAILS

Whole genome sequencing and analysis

The full GCRV-DY197 genome was sequenced using Illumina Sequencers (Illumina, USA) combined with a SMARTer RACE 5′/3′ Kit (Clontech, USA) following the guidelines provided by the manufacturer. All the sequencing results were assembled using SEQMAN software. And phylogenetic tree was generated using the Clustal W algorithm and the Neighbor-Joining (N-J) method, utilizing the amino acid sequence of the VP6 protein. The other GCRV genomes were obtained from the GenBank database. The above required primers are shown in key resources table.

Regression infection experiment

The 20 healthy grass carp and 20 rare minnows were injected with 200 μL and 20 μL volumes of GCRV-DY197 (1×10^6 copies/μL),[49] respectively, with the same volume in sterile PBS as a control. The water temperature was maintained at 28°C for the experiment and fish mortality was recorded daily.

GCRV-DY197 proliferation *in vitro* and *in vivo*

A total of 50 healthy grass carp and grass carp liver cells (L8824) were infected with 1×10^6 copies/μL of GCRV-DY197. The infected L8824 cells and the organs from infected grass carp were collected daily for seven days. The entire RNA was isolated from the tissue and cell samples using TRIzol reagents (Invitrogen, USA), and then cDNA was synthesized following the manufacturer's instructions with the EasyScriptOne-Step gDNA Removal and cDNA Synthesis SuperMix Kit (TransGen Biotech). The proliferation of GCRV-DY197 in grass carp tissues and liver cells was analyzed via three-time real-time quantitative PCR (qPCR) using TB GreenPremix Ex Taq II (Takara, Japan). The standard curve was constructed using segment S2 that based on previous research (Figure S1).[50]

Real-time quantitative PCR

Spleen cDNA samples were obtained and the transcriptional levels of interferon (IFN), immunoglobulin M (IgM), interferon-induced Mx protein (Mx), and histocompatibility complex (MHC-I) in GCRV-DY197-infected grass carp were determined using qPCR. The qPCR was performed with a reaction mixture consisting of 10 μL TB GreenPremix Ex Taq II, 2 μL cDNA sample, 0.8 μL of each primer (10 μM), and ddH2O in a total volume of 20 μL. The relative mRNA expression levels of immune-related genes were determined as the fold change in comparison to β-actin expression using the $2^{-\Delta\Delta Ct}$ method. The above required primers are shown in key resources table.[14,51]

Plasmid construction and transfection

The complete sequence of each viral gene was amplified via PCR, utilizing the cDNA derived from GCRV-DY197 as the template, and cloned into the pEGFP-N1 vector at the *BamH I* site. Recombinant plasmids with successful sequence validation were extracted with the endotoxin-free kit (Omega, USA), and a total of 14 μg plasmids were transfected into GCO cells. After transfecting for 48 h, the GCO cells were collected for the subsequent research.

Subcellular localization

The GCO cells transfected with recombinant plasmids were cultured in confocal petri dishes. After being rinsed with PBS, the cells were treated with 300 μL of 4% paraformaldehyde for 25 min, followed by staining with 300 μL of DAPI solution for 10 min in dark conditions. Subsequently, the staining solution was removed, and the cells were immersed in PBS for observation using a confocal microscope (Olympus, Japan).

Protein extraction

The GCO cells transfected with corresponding plasmids were collected by centrifugation (1,000 × g, 4°C, 5 min) after being washed with precooled PBS twice. Pellets were resuspended with cell lysis buffer and sonicated at 120 W on ice. The cell lysis buffer contained 20 mM HEPES (pH = 7.5), 150 mM NaCl, 1% N-Dodecyl-β-D-Maltoside, and 1 × Roche protease & phosphatase inhibitor cocktail. After incubation for 1 h on ice, cell debris was removed by centrifugation (12,000 × g, 4°C, 10 min).

Affinity purification mass spectrometry

The APMS experiment was based on our previous experimental procedure.[43] The lysates containing corresponding viral protein were incubated with an anti-GFP antibody that bound to Protein A Magnetic Beads for 1 h. After the beads were washed with PBS five times to remove the dissociated proteins, the target protein complexes were released using 0.1 M glycine buffer (pH = 2–3) and neutralized with 1 M Tris buffer (pH = 8.5) at the ratio of 1:10. Afterward, the eluate was subjected to denaturation at 95°C for 10 min, followed by reduction using 10 mM freshly prepared DTT, alkylation with 15 mM iodoacetamide in the absence of light, and digestion with trypsin at 37°C overnight. All samples were purified using Zip Tip C18 plates according to the manufacturer's instructions and reconstituted in 0.1% formic acid for MS analysis. The APMS experiment for each viral protein was repeated twice.

The samples were analyzed by a Q-Exactive Plus mass spectrometer equipped with an EASY-nLC 1200 system (Thermo Fisher Scientific), in which the peptides were separated using a C18 nanotrap column and ionized at 2.2 kV. The MS detection parameters were set as follows: a Data Dependent Acquisition (DDA) was used to acquire the MS/MS spectra of the top 20 most-abundant precursor ions; 5×10^4 ions were accumulated with a 50 ms maximum ion injection period for MS/MS analysis; isolation width was 1.8 m/z; the dynamic exclusion period was 40 s; the normalized HCD collision energy was set as 28%.

QUANTIFICATION AND STATISTICAL ANALYSIS

Three independent experimental replicates were performed for all experiments unless otherwise stated.